

# CELL TRANSPLANTATION

The Regenerative Medicine Journal

## FIGURE LEGENDS

**Figure 1.** *In vitro* cytotoxicity assay of neutrophil elastase against islets and optimum concentration of sivelestat in ET-Kyoto solution. (A) The cytotoxicity of neutrophil elastase against islets and the inhibitory effects of sivelestat were assessed by LDH assay. Data are mean±SD of three independent experiments. \* $p<0.05$ , \*\* $p<0.01$ . (B) Islet yields under various concentrations of sivelestat. Data are mean±SD of three independent experiments. \* $p<0.05$ .

**Figure 2.** Accumulation of activated neutrophils in the pancreas and neutrophil elastase activity during islet isolation. (A) Representative histology of the pancreas before and at the end of warm digestion. Activated neutrophils are stained red-brown (black arrow) by naphthol AS-D chloroacetate esterase. Calibration bars=100  $\mu\text{m}$ . (B) Number of activated neutrophils per field (magnification,  $\times 100$ ) was counted under microscopy. Data are mean±SD of five sections. \*\* $p<0.01$ , \*\*\* $p<0.001$ . (C) Neutrophil elastase activity in the supernatant during islet isolation measured at various time points of islet isolation (before warm digestion, at the end of warm digestion, after purification). All experiments were done using each independent mouse. One mouse was used in each experiment ( $n=1$ ). Data are mean±SD of five independent samples. \*\*\* $p<0.001$ .

**Figure 3.** Assessment of apoptosis during islet isolation by TUNEL staining. (A) Representative histological sections of the islets at the end of warm digestion. Note the

brown TUNEL-stained apoptotic cells (arrowhead). Calibration bars = 100  $\mu$ m. (B)

The density of TUNEL-positive cells (cells/islet), was determined under  $\times$  400 magnification. All experiments were done using each independent mouse. One mouse was used in each experiment (n=1). Data are mean $\pm$ SD of five independent sections. \*\*\* p<0.001.

**Figure 4.** Results of islet isolation according to the type of isolation solution. (A) Size distribution for each diameter (50-150, 150-250, 250-350, 350-  $\mu$ m) of isolated islets assessed by using each isolation solution. All experiments were done using each independent mouse. One mouse was used in each experiment (n=1). Data are the mean percentage from five independent experiments. (B) Representative microscopic images of the islets immediately after isolation. The morphology of isolated islets was observed by scanning electron microscopy. Calibration bars= 100  $\mu$ m.

**Figure 5.** *In vitro* viability assay of isolated islets by TMRE and 7-AAD. *Top panel:* Representative flow cytometry analysis by TMRE assay. *Bottom panel:* Representative flow cytometry analysis by 7-AAD. Percentage data represent percentages of cells with high fluorescence.

**Figure 6.** *In vitro* viability assay of isolated islets by MTS. (A) Viability of fresh islets (30 cells) was assessed using MTS assay. Data are mean $\pm$ SD of five independent experiments. \* p<0.05. (B) Isolated islets (30 cells) were cultured for 0, 1, 2 days and

their viabilities were assessed by MTS assay. Data are mean±SD of five independent experiments. \*  $p < 0.05$ , \*\*  $p < 0.01$  versus fresh islets

**Figure 7.** Results of *in vivo* transplant experiments. Islets were isolated using one of the isolation solutions (ET-Kyoto, S-Kyoto), then immediately transplanted (500 allogeneic islets) under the kidney capsule of diabetic mice. Sivelestat was injected intraperitoneally at 2 mg/day at 1 day before transplantation and every day until posttransplantation day 14. (A) Blood glucose levels of recipient mice transplanted with the islets. Data are mean±SD of five independent mice. (B) Serum neutrophil elastase activity of recipient mice was measured at day 1 before transplantation and days 4, 7, 14, 21, 28 post-transplantation. Data are mean±SD of three independent samples. \*  $p < 0.05$ , versus S-Kyoto. (C) IPGTT of recipient mice was performed at posttransplantation day 7. Blood glucose was measured in each group (non-diabetic wild-type mice, untreated diabetic mice, recipient mice transplanted with islets isolated by the use of ET-Kyoto, S-Kyoto, and S-Kyoto with sivelestat) before injection and at 15, 60, 120 min after injection. Data are mean±SD of three independent mice. (D) Immunohistochemical analysis of insulin in a representative mouse kidney engrafted with islets was performed at posttransplantation day 7. Calibration bars = 100  $\mu\text{m}$ .

**Figure 8.** Assessment of proinflammatory cytokines in isolation solution during islet isolation. The levels of proinflammatory cytokines (IL-2, 4, 6, 10, 17A, IFN- $\gamma$ , TNF- $\alpha$ ) in the isolation solution were measured during islet isolation (before warm digestion,

at the end of warm digestion, after purification). Data are mean±SD of four independent experiments. \* p<0.05.

**Figure 9.** Assessment of proinflammatory cytokines in sera of islet mouse recipients after islet transplantation (ITx). The levels of proinflammatory cytokines (IL-2, 4, 6, 10, 17A, IFN- $\gamma$ , TNF- $\alpha$ ) in the sera of islet recipients were measured at pretransplantation day 1 and posttransplantation days 4, 7, 14, 21, and 28. Data are mean±SD of three independent samples. \*\* p<0.01, versus non-sivelestat ip group, # p<0.05 and ## p<0.01, versus before transplantation (day -1).

CELL  
TRANSPLANTATION  
The Regenerative Medicine Journal

**Table 1.** Results of islet isolation according to the isolation solution

	UW	S-UW	ET-Kyoto	S-Kyoto
Islet count after purification (cells/mouse)	248±92*	270±121	280±86	332±74
IEQ after purification	243±68 <sup>§</sup>	276±126 <sup>¶</sup>	367±70*	651±52
Recovery rate of purification	55.8±10.4 <sup>¶</sup>	56.6±12.7*	56.6±4.6*	76.0±5.2
Isolation index	1.18±0.21 <sup>§</sup>	1.20±0.38 <sup>¶</sup>	1.56±0.21*	2.05±0.17
Islet purity (%)	82.7±3.1 <sup>§</sup>	84.0±2.2 <sup>¶</sup>	87.3±2.7	91.3±1.9

Data are expressed as mean±SD of five independent experiments.

\*p<0.05, <sup>¶</sup>p < 0.01, <sup>§</sup>p<0.001, compared with S-Kyoto isolation solution.

Islet count and purity were measured by the VH-analyzer software. Isolation index was calculated as the ratio of IEQ to islet count.

The recovery rate of purification (%) = IEQ after purification / IEQ before purification ×100

IEQ, islet equivalents; UW, University of Wisconsin

**Table 2.** Insulin concentration under low (2.8mM) and high (20mM) glucose and stimulation index according to the isolation solution used in the present study

	UW	S-UW	ET-Kyoto	S-Kyoto
Insulin concentration ( $\mu\text{g/l}$ ) under:				
low glucose (2.8 mM)	2.89 $\pm$ 0.37	2.75 $\pm$ 0.44	2.90 $\pm$ 0.30	2.98 $\pm$ 0.37
high glucose (20 mM)	3.68 $\pm$ 0.52 <sup>¶</sup>	3.64 $\pm$ 0.54 <sup>¶</sup>	3.78 $\pm$ 0.44 <sup>¶</sup>	4.46 $\pm$ 0.79
Stimulation Index (SI)	1.30 $\pm$ 0.06 <sup>§</sup>	1.31 $\pm$ 0.12 <sup>§</sup>	1.38 $\pm$ 0.12*	1.49 $\pm$ 0.08

Data are expressed as mean $\pm$ SD of five independent experiments.

\*p<0.05, <sup>¶</sup>p<0.01, <sup>§</sup>p<0.001, compared with the S-Kyoto solution.

SI was calculated as the ratio of insulin released during exposure to high glucose over the insulin released during low glucose incubation.

SI, Stimulation Index; UW, University of Wisconsin

**Table 3.** Survival of islet allografts in mice with streptozotocin-induced diabetes.

	without intraperitoneal injection of sivelestat		with intraperitoneal injection of sivelestat	
	ET-Kyoto	S-Kyoto	ET-Kyoto	S-Kyoto
Graft survival (days)	6, 7, 7, 8, 9	10, 10, 11, 12, 13	12, 13, 14, 17, 20	18, 19, 20, 22, 26
Mean Survival (days)	7.4±1.1	11.2±1.1 <sup>¶</sup>	15.2±3.3 <sup>§</sup>	21.0±3.2 <sup>†</sup>

Data are mean±SD of five independent experiments.

<sup>¶</sup>p<0.01, <sup>§</sup>p<0.001, compared with the ET-Kyoto isolation solution.

<sup>†</sup>p<0.001, compared with the S-Kyoto isolation solution.

CELL  
TRANSPLANTATION  
The Regenerative Medicine Journal

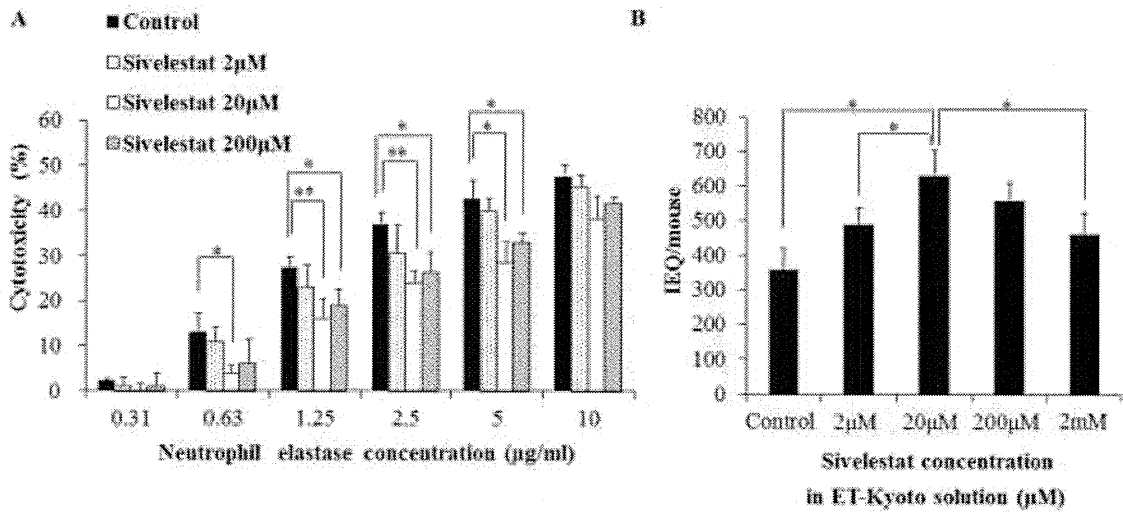


Figure 1

CELL  
TRANSPLANTATION  
The Regenerative Medicine Journal

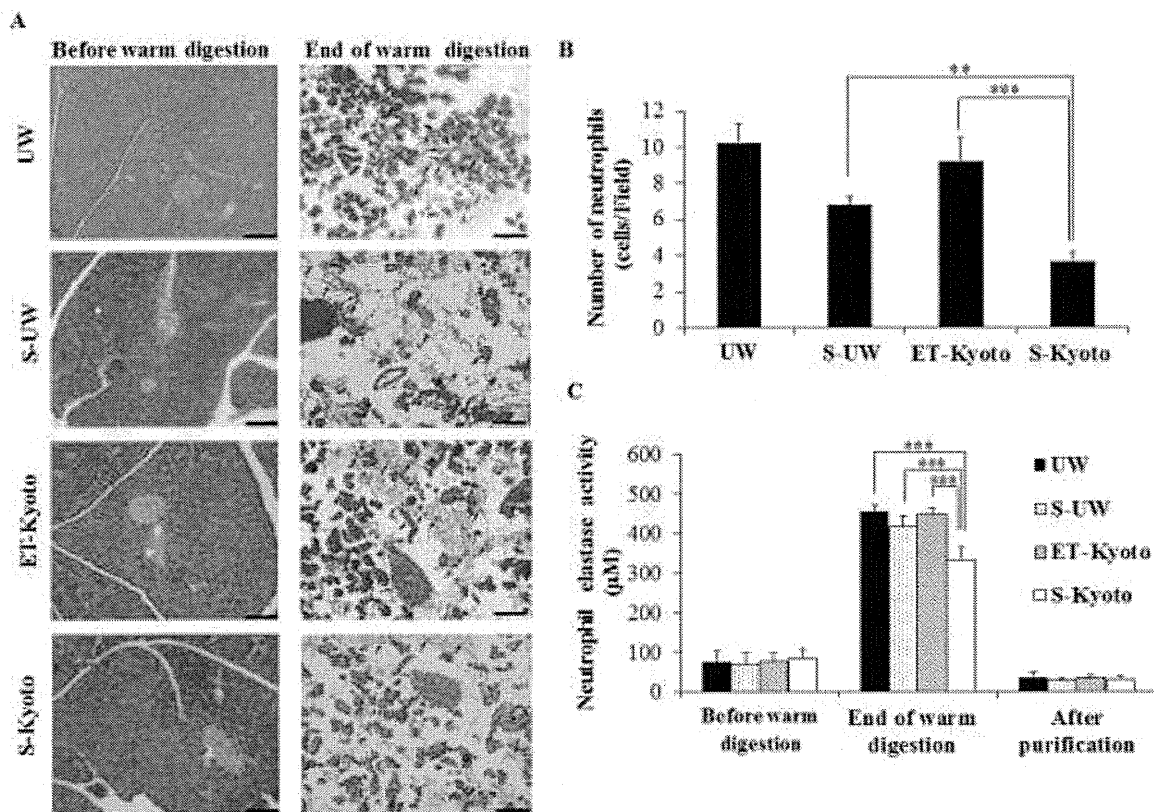


Figure 2

CELL  
TRANSPLANTATION  
The Regenerative Medicine Journal

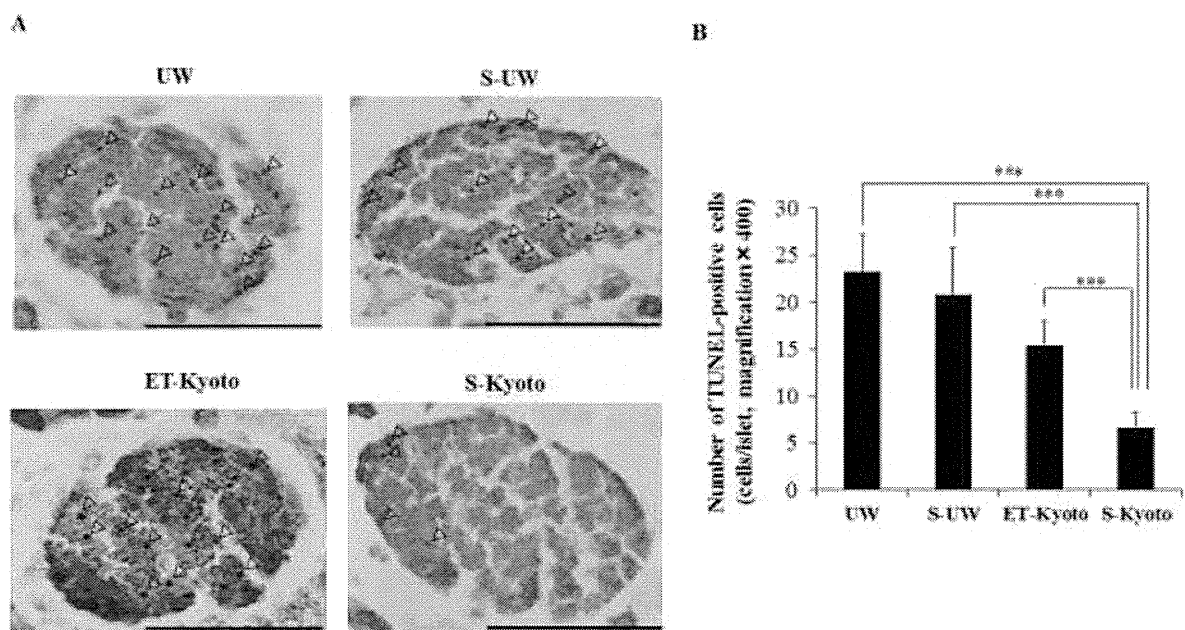


Figure 3

CELL  
TRANSPLANTATION  
The Regenerative Medicine Journal

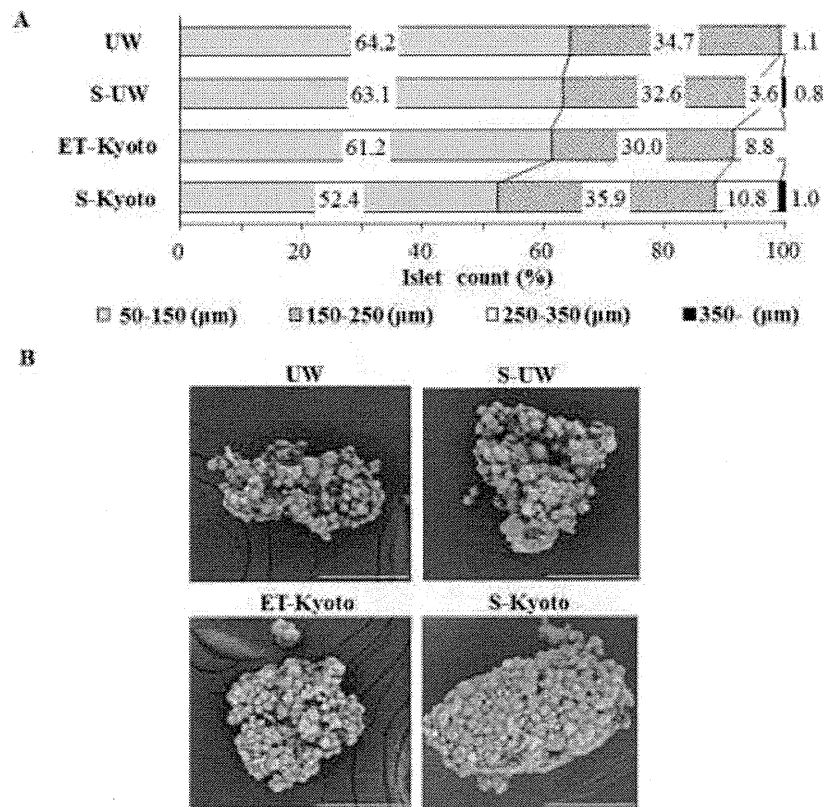


Figure 4

CELL  
TRANSPLANTATION  
The Regenerative Medicine Journal

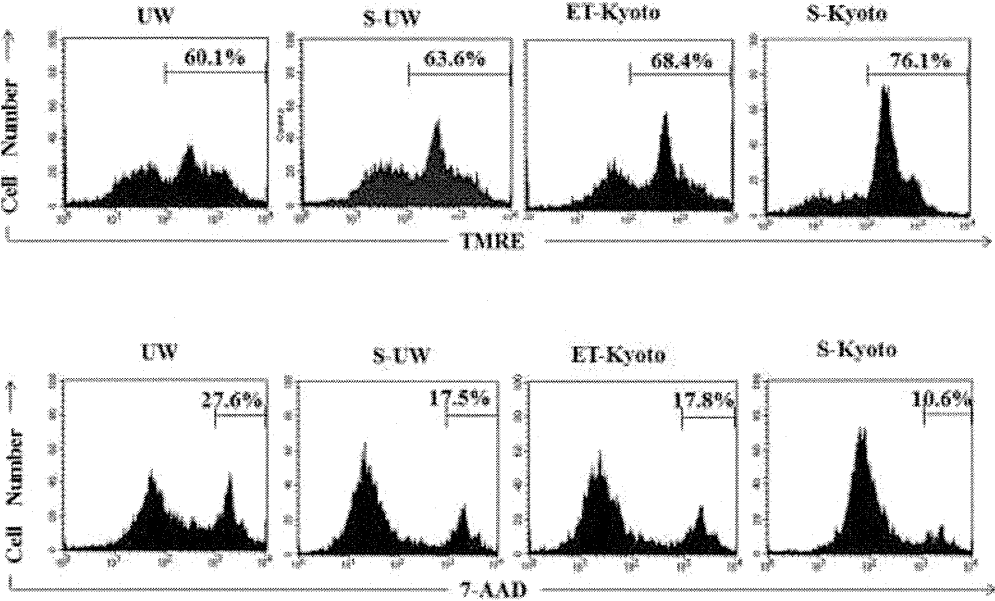


Figure 5

CELL  
TRANSPLANTATION  
The Regenerative Medicine Journal

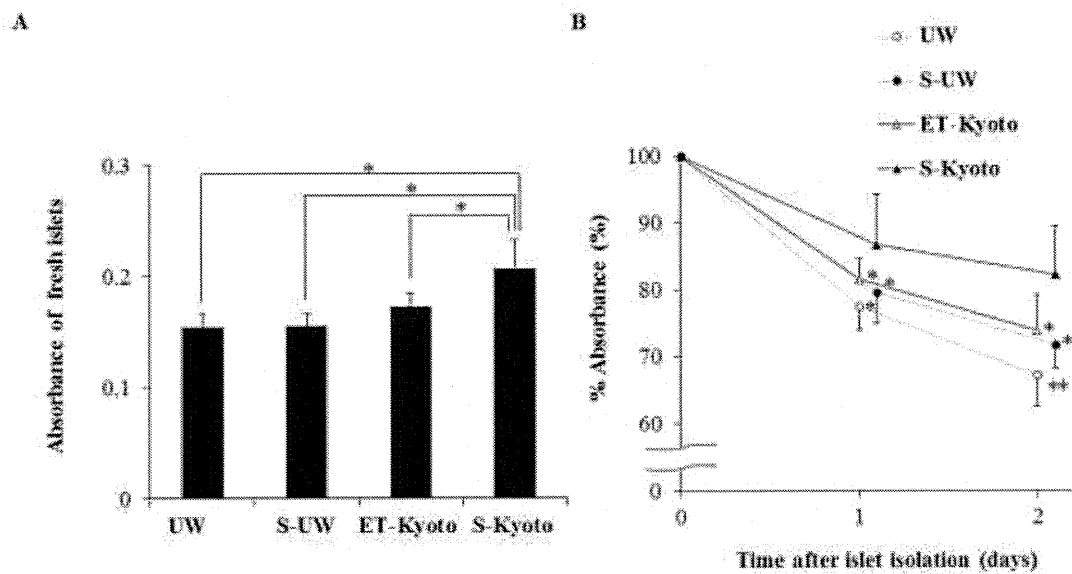


Figure 6

TRANSPLANTATION  
The Regenerative Medicine Journal

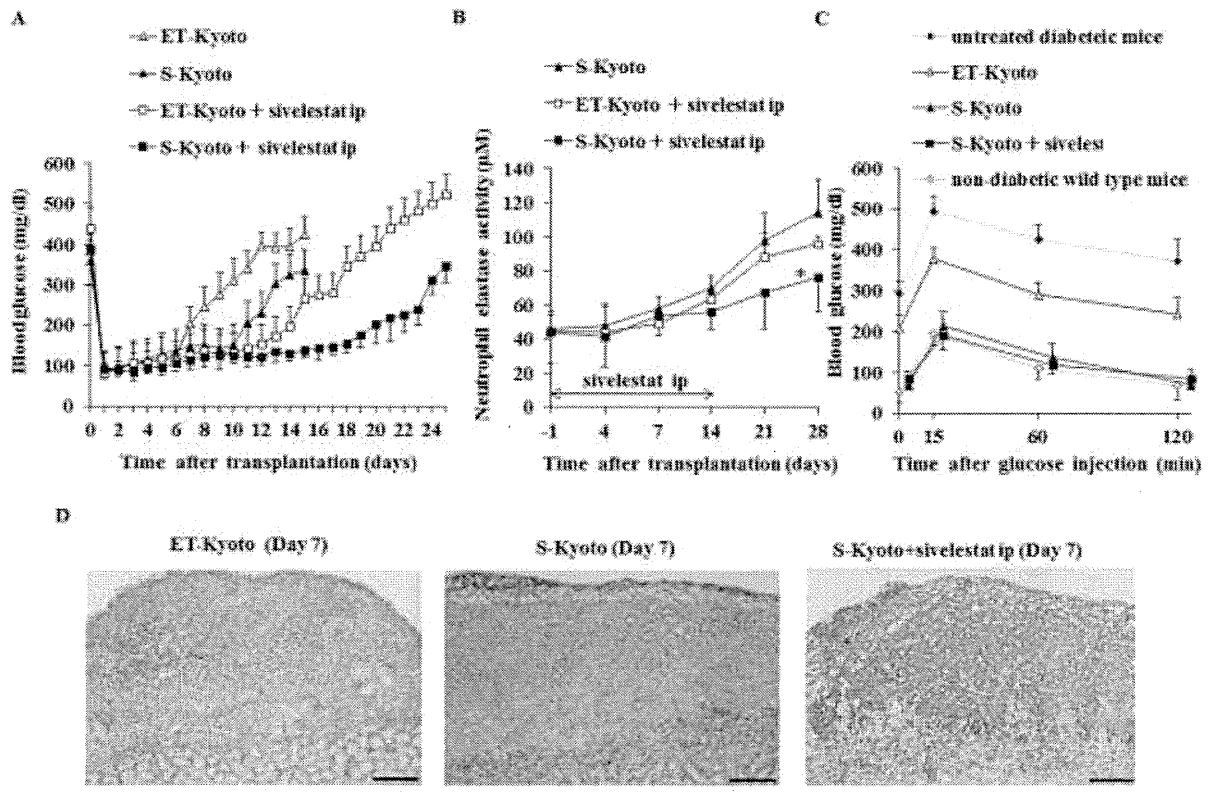


Figure 7

CELL  
TRANSPLANTATION  
The Regenerative Medicine Journal

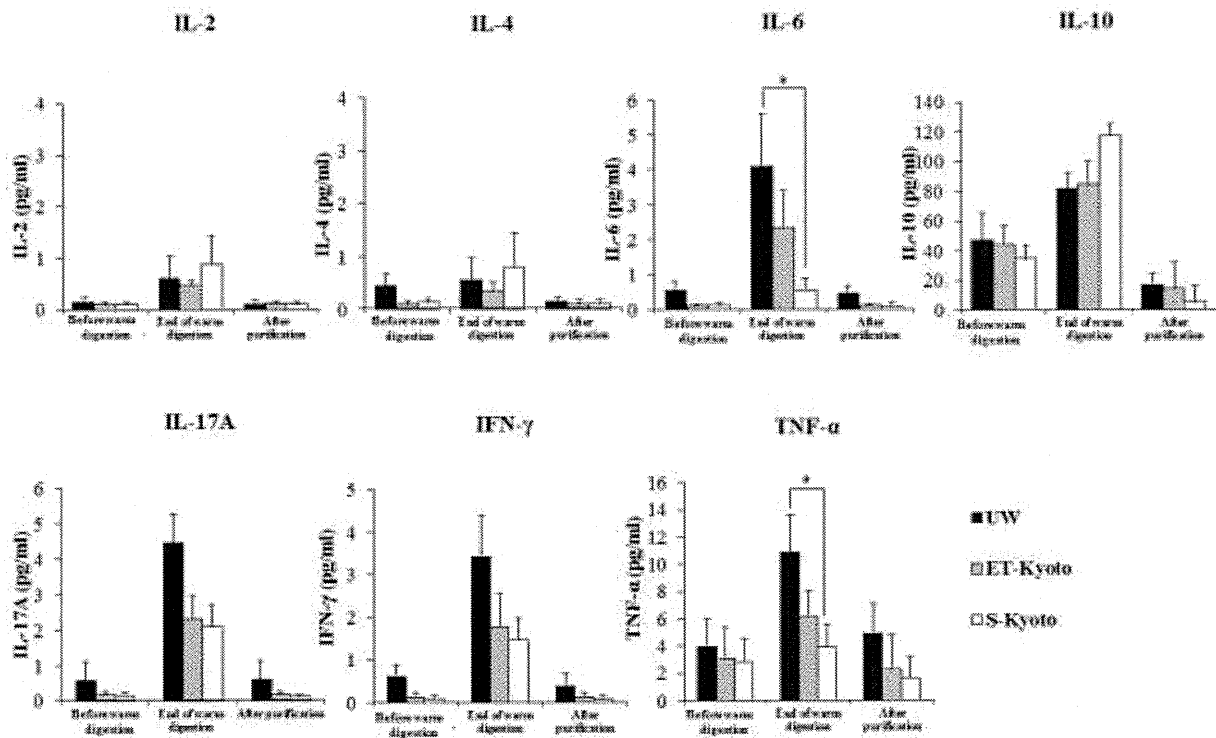


Figure 8

CELL TRANSPLANTATION  
The Regenerative Medicine Journal

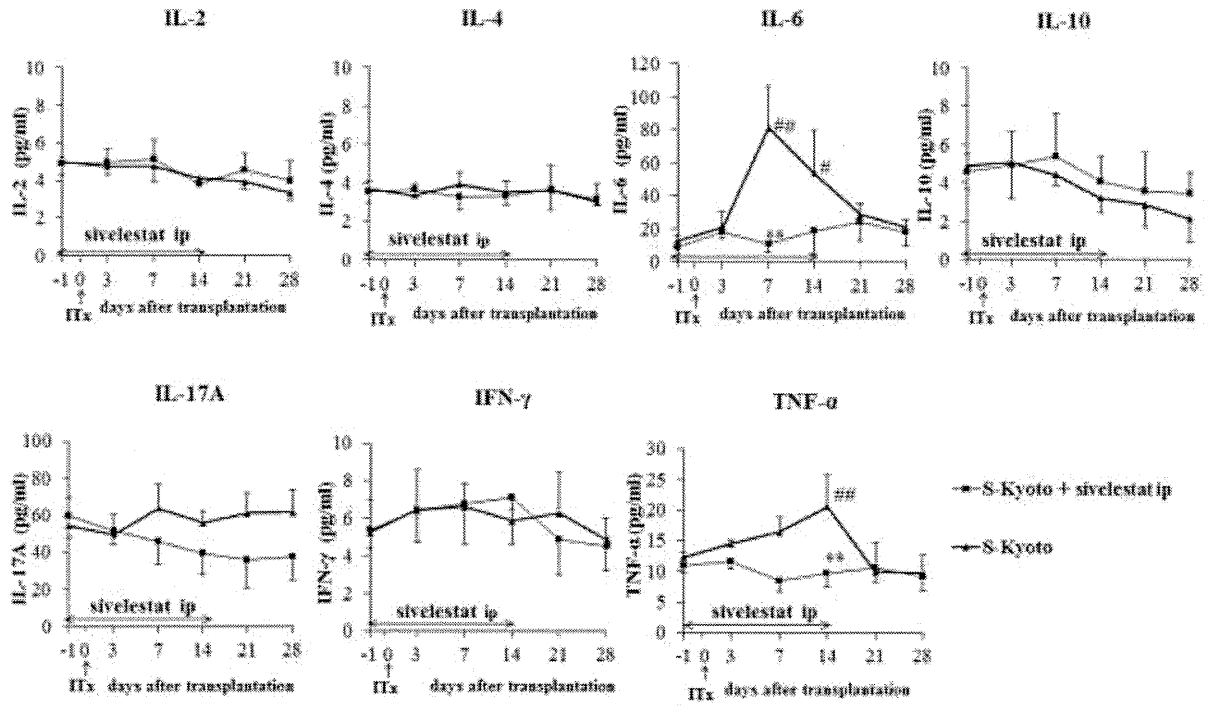


Figure 9

CELL  
TRANSPLANTATION  
The Regenerative Medicine Journal

## Tissue engineered myoblast sheets improved cardiac function sufficiently to discontinue LVAS in a patient with DCM: report of a case

Yoshiki Sawa · Shigeru Miyagawa · Taichi Sakaguchi · Tomoyuki Fujita · Akifumi Matsuyama · Atsuhiko Saito · Tatsuya Shimizu · Teruo Okano

Received: 15 August 2010 / Accepted: 31 January 2011 / Published online: 27 December 2011  
© Springer 2011

**Abstract** Dilated cardiomyopathy (DCM) is a heart muscle disease characterized by progressive heart failure, and is a leading cause of mortality and morbidity. Recently, cellular therapy for end-stage heart failure has been emerging. We herein report a 56-year-old male who received a transplant of autologous myoblast sheets manufactured in temperature-responsive culture dishes. His clinical condition improved markedly, leaving him without any arrhythmia and able to discontinue using a left ventricular assist system and avoid cardiac transplantation. These findings suggest that cellular therapy using myoblast sheets is a promising new strategy for treating patients with end-stage DCM. This method might be an effective alternative to heart transplantation in the near future.

**Keywords** Cell · DCM · Tissue engineering · LVAD

### Introduction

We herein report a patient with dilated cardiomyopathy (DCM) who received a transplant of autologous myoblast

sheets that were manufactured using temperature-responsive culture dishes. After the treatment, the patient was able to discontinue using a left ventricular assist system (LVAS). This novel method represents a promising strategy for clinical myocardial cellular therapy in patients with end-stage DCM.

### Case report

A 56-year-old male, who was suffering from idiopathic DCM (Fig. 2h), was referred to Osaka University Hospital under intra-aortic balloon pump (IABP) support, oxygenation with a respirator, portable cardiopulmonary bypass, and continuous venovenous hemodiafiltration (CVVHD). Upon admission, he received an implantation of an extracorporeal pneumatic LVAS (Toyobo, Tokyo, Japan) and RVAS-ECMO using a centrifugal pump. At 7 and 8 months after admission, he was examined to determine whether the LVAS could be discontinued. Before LVAD implantation, his ejection fraction (EF) was 11%. After LVAD implantation, an off-pump test revealed that his EF was 20%. Therefore, LV unloading by LVAD implantation had improved the cardiac function, but the results did not meet the criteria for LVAS explantation as described by Dandel et al. [1], and we judged that it was inadvisable to explant the LVAS at that time.

Myoblast cell sheet transplantation for this patient was approved by the Ethical Committee and Internal Review Board of Osaka University. Upon granting his informed consent, the patients had an approximately 10-g piece of skeletal muscle excised from his medial vastus muscle under general anesthesia. The autologous myoblasts derived from this muscle were cultured according to published procedures [2], grown to  $3 \times 10^8$  cells (more than

Y. Sawa (✉) · S. Miyagawa · T. Sakaguchi · T. Fujita  
Department of Cardiovascular Surgery, Osaka University  
Graduate School of Medicine, 2-2 Yamada-oka,  
Suita, Osaka 565-0871, Japan  
e-mail: sawa@surg1.med.osaka-u.ac.jp

A. Matsuyama · A. Saito  
Medical Center of Translational Research, Osaka University  
Graduate School of Medicine, Suita, Japan

T. Shimizu · T. Okano  
Tokyo Women's Medical University Institute of Advanced  
Biomedical Engineering and Science, Tokyo, Japan

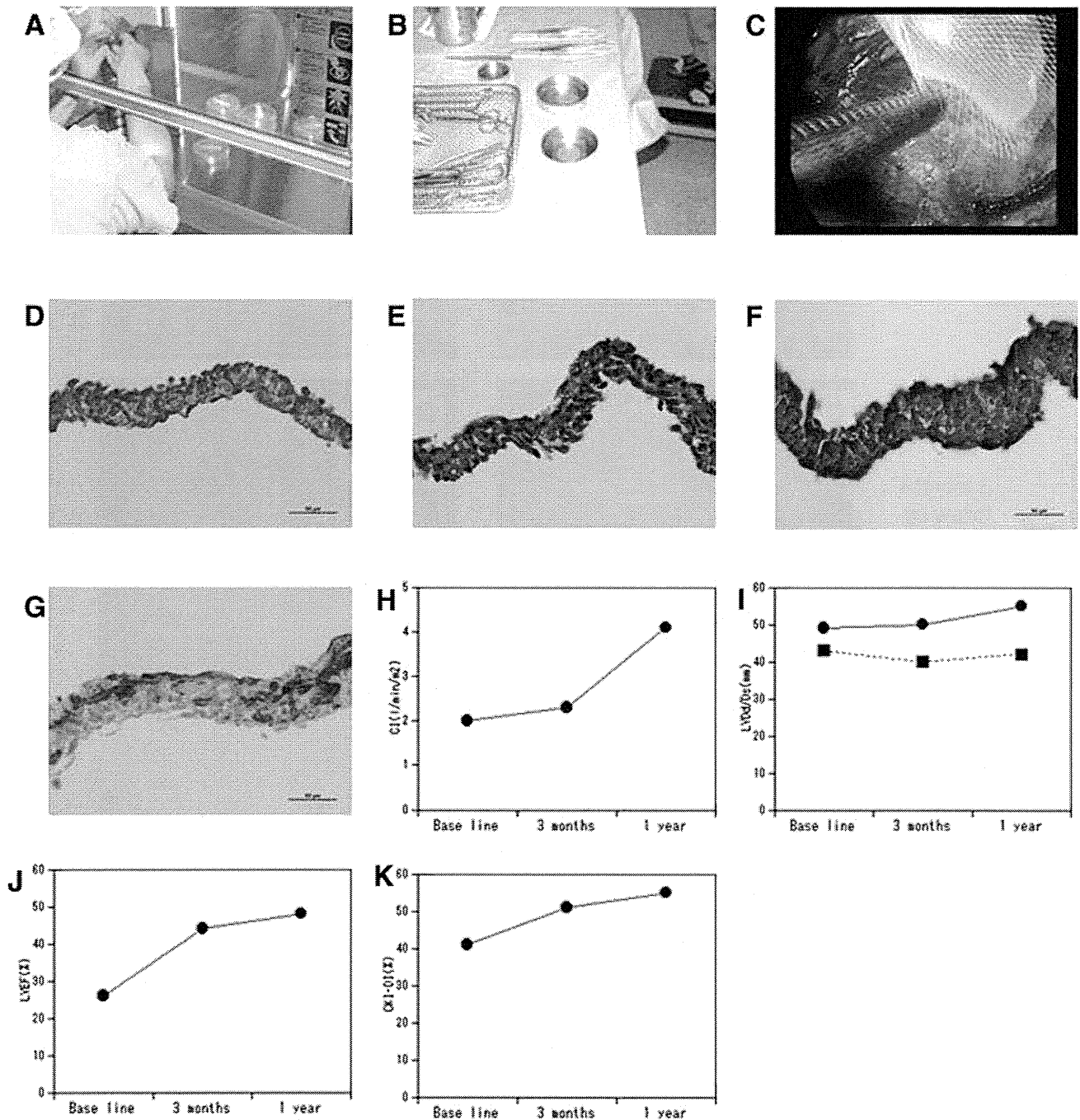


**Fig. 1** The histology of the myoblast sheet and the changes in hemodynamic variables from baseline (before myoblast sheet implantation), and at 3 months and 1 year follow-up examinations. Hemodynamic variables at baseline and at the 3-month follow-up were obtained at the examination for LVAS removal. **a, b** Preparation of myoblast sheets in the operating room. **c** Implantation of a myoblast sheet via a left lateral thoracotomy. **d** HE staining of a myoblast sheet; the myoblast sheet included many cells, and its

thickness was about 50  $\mu\text{m}$ . **e** Masson-Trichrome staining; the myoblast sheet consisted of cells and extracellular matrix. **f** Desmin staining; nearly all of the cells in the myoblast sheets were Desmin positive. **g** Alpha-myosin heavy chain staining; some cells in the myoblast sheets were Alpha-myosin heavy chain positive. **h** Cardiac index. **i** LVEDd (solid line) and LVEDs (dotted line). **j** LV ejection fraction. **k** Color kinesis diastolic indices (CK-DI)

90% purity by FACS analysis with CD56) for 3 weeks, and seeded onto temperature-responsive culture dishes. They formed cell sheets after 48 h, as previously reported. The

diameter of the myoblast sheet was about 4 cm and was round in shape. We implanted 4-layered myoblast sheets on one site and a total of 20 myoblast sheets (on five sites) to

